

# PHASE PORTRAITS OF A SIR EPIDEMIC MODEL

JAUME LLIBRE<sup>1</sup> AND TAYEB SALHI<sup>2</sup>

ABSTRACT. In this paper we classify the phase portraits of a SIR epidemic dynamics model. Depending on the values of the parameters this model can exhibit seven different phase portraits. In particular, from a biological point of view we prove that the unique attractors of this model are one or two equilibrium points depending on the values of the parameters, and from the phase portraits follow the basins of attraction of these equilibria.

## 1. INTRODUCTION AND STATEMENT OF THE MAIN RESULTS

The study of a widespread occurrence of an infectious disease in a community at a particular time has great importance, through decades many models have emerged to give explication for the spread and reason of epidemic outbreaks. The SIR [8] is one of the very realistic models that gives a good explanation of the spread of infectious disease which is used to study many epidemics like cholera [12], malaria [1] and very recently the novel coronavirus (2019-nCoV or COVID-19) which has been a great worry around the globe, thus scholars have focused their energies in studying the behavior of such fatal disease [3, 5, 13, 14].

In the SIR infections disease model, the total population  $N$  is composed of three groups of individuals which are:  $S(t)$  denote the number of members of a population susceptible to the disease at time  $t$ ;  $I(t)$  represents the number of infective members, and  $R(t)$  denotes the number of members who have been removed from the population (see [2, 4, 6]). The SIRS [4] model is a SIR model, which allows recovered individuals to return to a susceptible state, in the case when this model has birth rate and death rate can be written as

$$(1) \quad \begin{aligned} \frac{dS}{d\tau} &= -IH(I, S) - r_2S + r_1R + B(N), \\ \frac{dI}{d\tau} &= IH(I, S) - (r_2 + \nu)I, \\ \frac{dR}{d\tau} &= \nu I - (r_2 + r_1)R, \end{aligned}$$

where

- $H(I, S)$  is th nonlinear incidence rate concerning  $S$  and  $I$ ;
- $r_2$  is the common natural death rate of the three groups ( $S$ ,  $I$  and  $R$ );
- $B(N)$  denotes the birth rate and is a function depending on  $N = S + I + R$ ;

---

2010 *Mathematics Subject Classification.* Primary 34C05, 34A34.

*Key words and phrases.* Polynomial differential systems, equilibrium points, phase portraits, Hopf bifurcation, limit cycles, SIR epidemic dynamics model.

- $v$  is rate of the removal at which the infective individuals go into the removed class; and
- $r_1$  is the probability of which individuals in the removed class loss their immunity and go into the susceptible class.

Here  $N$  is the total population, and it is assumed in this model that all the new born infants are all susceptible (see [16]).

By doing same calculations and assumptions as in [16] we reduce system (1) to a two dimensional system. So by collecting the two sides of the equations of system (1) we get

$$\frac{dN}{dt} = B(N) - r_2N.$$

We suppose that this equation has an equilibrium point  $N_0$  satisfying  $B(N_0) = r_2N_0$ , and this equilibrium is asymptotically stable and unique when  $N_0 > 0$ . This assumption means that the total population will still in equilibrium while epidemic is spreading, so we can consider (1) just in the case  $S + I + R = N_0$ , and thus system (1) can be transformed into

$$(2) \quad \frac{dI}{d\tau} = IH(I, N_0 - I - R) - (r_2 + \nu)I, \quad \frac{dR}{d\tau} = \nu I - (r_2 + r_1)R.$$

Further a more special case has been brought forward [4, 10, 11, 15] by setting  $H(I, S) = KIS$  and  $r = \nu/(r_2 + \nu)$ ,  $h = \nu/(r_2 + r_1)$ ,  $a = K/(r_2 + \nu)$ ,  $t = (r_2 + \nu)\tau$ , with  $K > 0$ . Then the model (2) admits the following simpler form:

$$(3) \quad \frac{dI}{dt} = aI^2(N_0 - I - R) - I, \quad \frac{dR}{dt} = r\left(I - \frac{R}{h}\right).$$

We rescale the variables of system (3) in order to reduce the number of its parameters by doing the following change of variables  $I = \alpha x$ ,  $R = \beta y$ ,  $T = \gamma t$ . Then system (3) becomes

$$(4) \quad \dot{x} = a\alpha\gamma Nx^2 - a\alpha^2\gamma x^3 - a\alpha\beta\gamma x^2y - \gamma x, \quad \dot{y} = \frac{\alpha\gamma r}{\beta}x - \frac{\gamma r}{h}y.$$

Taking  $\alpha = \frac{r}{ahN}$ ,  $\beta = \frac{r}{aN}$ ,  $\gamma = \frac{h}{r}$ , system (4) writes

$$(5) \quad \dot{x} = -\frac{r}{ahN^2}x^3 - \frac{r}{aN^2}x^2y + x^2 - \frac{h}{r}x, \quad \dot{y} = x - y.$$

We rename the parameters  $b = h/r$ ,  $c = r/(ahN^2)$ , and  $d = r/(aN^2)$ . So the differential system (5) only depends now of three parameters and it becomes

$$(6) \quad \dot{x} = -bx - cx^3 - dx^2y + x^2, \quad \dot{y} = x - y,$$

where  $b$ ,  $c$  and  $d$  are positive parameters.

The objective of this paper is to study the phase portraits in the Poincaré disc of system, and in particular determine its attractors, the important objects in biology.

System (6) is defined in the plane  $\mathbb{R}^2$ , but in order to control its orbits which escape or come from infinity we extend it to the Poincaré disc. Roughly speaking the Poincaré disc  $\mathbb{D}$  is the closed unit disc centered at the origin of coordinates of  $\mathbb{R}^2$ , the interior of  $\mathbb{D}$  is identified with  $\mathbb{R}^2$  and its boundary, the circle  $\mathbb{S}^1$  is identified with the infinity of  $\mathbb{R}^2$ . Note that in the plane  $\mathbb{R}^2$  we can go to infinity in

as many directions as points has the circle. For more details on the Poincaré disc see Chapter 5 of [7].

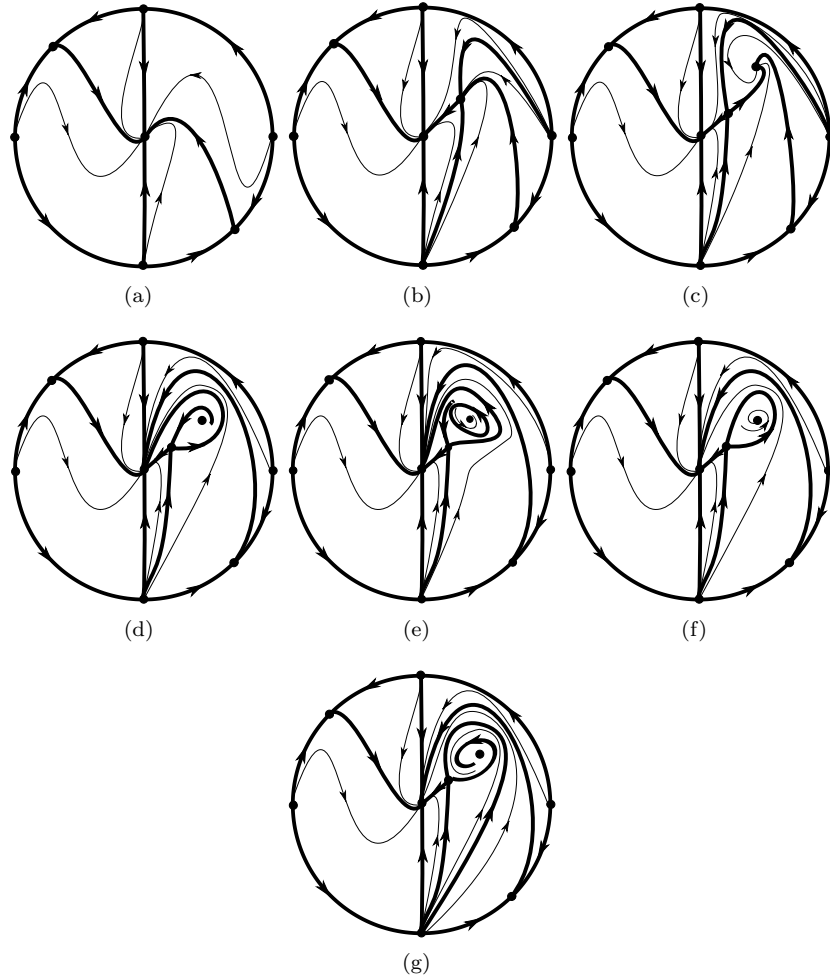


FIGURE 1. All topologically different phase portraits in the Poincaré disc of system (6).

Our main result is the following.

**Theorem 1.** *The phase portraits in the Poincaré disc of systems (6) are topologically equivalent to one of the phase portraits given in Figure 1.*

Theorem 1 is proved in section 4 assuming that the following conjecture holds. At this moment we only have numerical evidence that it must hold. It is well known that in general to prove the existence and uniqueness of a limit cycle is a very difficult problem.

**Conjecture.** *The differential system (6) has at most one limit cycle.*

A *limit cycle* of system (6) is a periodic orbit of this system isolated in the set of all periodic orbits of the system.

A key point in the proof of Theorem 1 is the study of the Hopf bifurcations of system (6). We recall that system (6) exhibits a Hopf bifurcation if it has an equilibrium point where the stability switches and a limit cycle arises.

**Theorem 2.** *System (6) when  $1 - 4b(c + d) > 0$  exhibits a Hopf bifurcation at the equilibrium point*

$$p_+ = \left( \frac{1 + \sqrt{1 - 4b(c + d)}}{2(c + d)}, \frac{1 + \sqrt{1 - 4b(c + d)}}{2(c + d)} \right).$$

if and only if

$$b > 1, \quad 0 < c < \frac{b-1}{4b^2} \quad \text{and} \quad d = d_0 = \frac{c(1-2b)}{b-1} + \sqrt{\frac{c}{b-1}}.$$

Moreover an unstable limit cycle bifurcates from this equilibrium point for values of  $d < d_0$  but sufficiently close to  $d_0$ .

Theorem 2 is proved in section 3.

## 2. EQUILIBRIUM POINTS AND THE HOPF BIFURCATION

The equilibrium points of system (6) and their local phase portraits are characterized in the next result.

**Proposition 3.** *The polynomial differential system (6) has*

- (a) *only one finite equilibrium point at the origin of coordinates if  $1 - 4b(c + d) < 0$ , which is a stable node;*
- (b) *two finite equilibrium points if  $1 - 4b(c + d) = 0$ , a stable node at the origin and a saddle-node at the point*

$$p_0 = \left( \frac{1}{2(c + d)}, \frac{1}{2(c + d)} \right);$$

- (c) *three finite equilibrium points if  $1 - 4b(c + d) > 0$  a stable node at the origin, and two additional equilibria at*

$$p_{\pm} = \left( \frac{1 \pm \sqrt{1 - 4b(c + d)}}{2(c + d)}, \frac{1 \pm \sqrt{1 - 4b(c + d)}}{2(c + d)} \right).$$

Moreover,  $p_-$  is a saddle, and  $p_+$  is either a node, or a focus, or a center.

*Proof.* The origin of coordinates always is a finite equilibrium point of system (6) and since the eigenvalues of the linear part of the system at the origin are  $-1$  and  $-b$ , the origin is a stable node.

Since it is easy to check that when  $1 - 4b(c + d) < 0$  system (6) has only one equilibrium, the origin of coordinates, statement (a) follows.

When  $1 - 4b(c + d) = 0$  system (6) has two finite equilibrium points the origin and the point  $p_0$  which is semi-hyperbolic, because the eigenvalues of the linear part of the system at this point are  $0$  and  $(d - 4(c + d)^2)/(4(c + d)^2) < 0$ . Using

Theorem 2.19 of the book [7] we obtain that  $p_0$  is a saddle-node. Statement (b) is proved.

If  $1 - 4b(c + d) > 0$  system (6) have three finite equilibrium points, the origin and  $p_{\pm}$ . The determinant of the matrix of the linear part of system (6) at  $p_{\pm}$  is

$$D_{\pm} = \frac{1 - 4b(c + d) \pm \sqrt{1 - 4b(c + d)}}{2(c + d)}.$$

Since the parameters  $b$ ,  $c$  and  $d$  are positive, it follows that  $0 < 1 - 4b(c + d) < 1$ , and consequently  $p_-$  is a saddle because  $D_- < 0$ , and  $p_+$  is either a node, or a focus, or a center because  $D_+ > 0$ , for more details see Chapter 2 of [7]. Hence statement (c) follows.  $\square$

We remark that from the proof of Theorem 2 it will follow that the equilibrium point  $p_+$  never will be a center.

For studying the infinite singular points in the Poincaré disc, we use the definitions and notations given in Chapter 5 of [7], then we have the following result.

**Proposition 4.** *The polynomial differential system (6) has*

- (a) *in the local chart  $U_1$  two equilibrium points, an unstable node at the origin and a semi-hyperbolic saddle at  $(-c/d, 0)$ , and*
- (b) *the local phase portrait at the origin of  $U_2$  inside the Poincaré disc and on the right of the invariant straight line  $x = 0$  has a hyperbolic sector, and on the left of  $x = 0$  has an unstable parabolic sector. Moreover, in the origin of  $V_2$  inside the Poincaré disc and on the left of the invariant straight line  $x = 0$  has a hyperbolic sector, and on the right  $x = 0$  has an unstable parabolic sector.*

*Proof.* The polynomial differential system (6) in the local chart  $U_1$  becomes

$$(7) \quad \dot{u} = cu + du^2 - uv + v^2 - uv^2 + buv^2, \quad \dot{v} = v(c + du - v + bv^2).$$

On the straight line  $v = 0$  system (7) have two equilibrium points the origin and the point  $(-c/d, 0)$ . Since the eigenvalues of the linear part of system (7) at the origin are  $c$  of multiplicity 2, then the origin is an unstable node. The eigenvalues of the linear part of system (7) at the point  $(-c/d, 0)$  are 0 and  $-c$ , then is a semi-hyperbolic equilibrium point. So we shall apply Theorem 2.19 of [7]. First, we translate the equilibrium point  $(-c/d, 0)$  at the origin of coordinates of the chart  $U_1$  therefore system (7) becomes

$$(8) \quad \begin{aligned} \dot{u} &= -cu + \frac{c}{d}v + du^2 - uv + \left(\frac{c - bc}{d} + 1\right)v^2 + (b - 1)uv^2, \\ \dot{v} &= duv - v^2 + bv^3. \end{aligned}$$

Moreover, by doing the change of variables  $Y = (c/d)v - cu$ ,  $X = v$  in system (8), and change the sign of time in order to apply Theorem 2.19 system (8) becomes

$$(9) \quad \begin{aligned} \dot{X} &= \frac{d}{c}XY - bX^3 = A(X, Y), \\ \dot{Y} &= cY - \left(\frac{bc^2 - c^2}{d} - c\right)X^2 + \frac{d}{c}Y^2 + (1 - b)X^2Y - \frac{c}{d}X^3 = cY + B(X, Y). \end{aligned}$$

So

$$Y = f(X) = \frac{bc - c - d}{d}X^2 + \frac{1}{d}X^3 + h.o.t.$$

is the solution of the equation  $cY + B(X, Y) = 0$  in a neighborhood of the point  $(0, 0)$  for system (9), as usual *h.o.t.* denotes higher order terms. By substituting  $Y = f(X)$  in the first equation of system (9) we get

$$g(X) = -\frac{c+d}{c}X^3 + \frac{1}{c}X^4 + h.o.t.$$

Therefore  $m = 3$  is odd and  $-(c+d)/c < 0$  by applying Theorem 2.19 of [7] we conclude that the equilibrium point  $(-c/d, 0)$  is always a saddle point. This completes the proof of statement (a).

The polynomial differential system (6) in the local chart  $U_2$  becomes

$$(10) \quad \dot{u} = -u(du + cu^2 - uv - v^2 + bv^2 + uv^2), \quad \dot{v} = (1-u)v^3.$$

The origin of the local chart  $U_2$  is a linearly zero singular point, we must study it doing blow ups. For that we do the change of variables  $(u, v) = (u, w = v/u)$ . Therefore, system (10) becomes

$$\dot{u} = -u^2(d + cu - uw - uw^2 + buw^2 + u^2w^2), \quad \dot{w} = uw(d + cu - uw + buw^2).$$

We eliminate the common factor  $u$  doing a scaling of the time and we get

$$(11) \quad \dot{u} = -u(d + cu - uw - uw^2 + buw^2 + u^2w^2), \quad \dot{w} = w(d + cu - uw + buw^2).$$

On the straight line  $u = 0$  there is a unique equilibrium point, the origin. Since the eigenvalues of the linear part of system (11) are  $d$  and  $-d$  the origin of this system is a saddle. Going back through the changes of variables and taking into account that the axes are invariant in the local chart  $U_2$ , we get the local phase portrait at the origin of  $U_2$  inside the Poincaré disc and on the right of the invariant straight line  $x = 0$  has a hyperbolic sector, and on the left of this invariant straight line has an unstable parabolic sector. Moreover, in the origin of  $V_2$  inside the Poincaré disc and on the left of the invariant straight line  $x = 0$  has a hyperbolic sector, and on the right of this invariant straight line has an unstable parabolic sector. So statement (b) is proved.  $\square$

### 3. PROOF OF THEOREM 2

In this section we shall study the existence of Hopf bifurcations for system (6).

The matrix of the linear part of system (6) at  $p_+$  is

$$\begin{pmatrix} \frac{4bc^2 + 2bd^2 - c(\sqrt{1 - 4b(c+d)} - 6bd + 1)}{2(c+d)^2} & -\frac{d(\sqrt{1 - 4b(c+d)} + 1)^2}{4(c+d)^2} \\ 1 & -1 \end{pmatrix}.$$

The eigenvalues of this matrix are

$$\begin{aligned} \lambda_{\pm} = & \frac{1}{4(c+d)^2} \left( 2(2b-1)c^2 + c((6b-4)d-1) + 2(b-1)d^2 - c\sqrt{1-4b(c+d)} \right. \\ & \pm \frac{1}{2} \left( 32(c+d)^3 \left( 4b(c+d) - 1 - \sqrt{1-4b(c+d)} \right) \right. \\ & \left. \left. + 4 \left( (2-4b)c^2 + c \left( \sqrt{1-4b(c+d)} + (4-6b)d + 1 \right) - 2(b-1)d^2 \right)^2 \right)^{\frac{1}{2}} \right). \end{aligned}$$

A Hopf bifurcation needs that these eigenvalues be purely imaginary numbers, and after tedious computations this occurs if and only if

$$(12) \quad b > 1, \quad 0 < c < \frac{b-1}{4b^2}, \quad d = d_0 = \frac{c(1-2b)}{b-1} + \sqrt{\frac{c}{b-1}},$$

if for these values of the parameters we do not have a center, there exists a Hopf bifurcation for system (6) because a change in the stability of the focus  $p_+$  takes place, and in such a case when  $d = d_0$  system (6) will exhibit a Hopf bifurcation. For more details on a Hopf bifurcation see for instance [9].

In order to check that for the values of the parameters (12) system (6) has not a center at the equilibrium point  $p_+$  we shall see that there is a nonzero Liapunov constant at  $p_+$ , and if it is nonzero this will prove that a limit cycle bifurcates from the equilibrium point  $p_+$  when the parameters  $(b, c, d)$  are on the Hopf bifurcation surface (12).

In order to simplify the computations for obtaining the Liapunov constants we eliminate the square roots in the equilibrium point and in their eigenvalues changing the parameters  $(b, c)$  by the new parameters  $(k, \omega)$  doing the following steps.

We eliminate the square root  $\sqrt{1-4b(c+d)}$  changing the parameter  $b$  by the new parameter  $k$  doing the change  $b = (1-k^2)/(4(c+d))$ . Thus the equilibrium point  $p_+$  becomes

$$\left( \frac{k+1}{2(c+d)}, \frac{k+1}{2(c+d)} \right).$$

We translate the equilibrium point  $p_+$  at the origin of coordinates by doing the change of variables

$$x = u + \frac{k+1}{2(c+d)}, \quad y = v + \frac{k+1}{2(c+d)}.$$

Then systems (6) becomes

$$(13) \quad \begin{aligned} \dot{u} = & -\frac{(k+1)(2ck+d(k-1))}{4(c+d)^2}u - \frac{d(k+1)^2}{4(c+d)^2}v - \frac{3ck+c+d(k-1)}{2(c+d)}u^2 \\ & - \frac{d(k+1)}{c+d}uv - cu^3 - dvu^2, \\ \dot{v} = & u - v. \end{aligned}$$

The matrix of the linear part of this system at the origin is

$$(14) \quad \begin{pmatrix} -\frac{(k+1)(2ck+d(k-1))}{4(c+d)^2} & -\frac{d(k+1)^2}{4(c+d)^2} \\ 1 & -1 \end{pmatrix}.$$

Now we change the parameter  $c$  by a new parameter  $L > 0$  taking  $c = (1 - 2k^2 + k^4 - L^2)/(16(1 + k)^2)$ . Then the matrix (14) becomes

$$M = \begin{pmatrix} 1 & \frac{3k^2 + 4k - L + 1}{k^2 + L - 1} \\ 1 & -1 \end{pmatrix},$$

and the eigenvalues of this matrix are

$$\lambda_{\pm} = \pm \frac{2\sqrt{k(k+1)}}{\sqrt{1 - k^2 - L}}i = \pm\omega i,$$

with  $\omega > 0$ , i.e. we change the parameter  $L$  by the new parameter  $\omega$  taking

$$L = \frac{\omega^2(1 - k^2) - k^2 - k}{\omega^2}.$$

With the new parameter  $\omega$  the computations of the Liapunov constants becomes shorter and clearer.

We shall write the matrix  $M$  in its real Jordan normal form

$$J = \begin{pmatrix} 0 & \omega \\ -\omega & 0 \end{pmatrix}.$$

For that we will do the change of variables

$$\begin{pmatrix} U \\ V \end{pmatrix} = \begin{pmatrix} 1 & 0 \\ \frac{1}{\omega} & -\frac{4\omega^2 + 1}{2\omega} \end{pmatrix} \begin{pmatrix} u \\ v \end{pmatrix},$$

and the differential system (13) in the new variables  $(U, V)$  writes

$$(15) \quad \begin{aligned} \dot{U} &= \frac{(kU + 4\omega^2)((k-1)U^2\omega + kUV + 4V\omega^2)}{16\omega^3}, \\ \dot{V} &= \frac{U(k^2UV + (k-1)kU^2\omega + 4(k-1)U\omega^3 + 8kV\omega^2 - 32\omega^5)}{32\omega^4}. \end{aligned}$$

We pass the differential system (15) to polar coordinates  $(r, \theta)$  through  $U = r \cos \theta$  and  $V = r \sin \theta$ , and we get

$$(16) \quad \begin{aligned} \dot{r} &= \frac{r^2 \cos \theta (2\omega \cos \theta + \sin \theta) ((k-1)\omega \cos \theta + 2k \sin \theta)}{8\omega^2} \\ &\quad - \frac{kr^3 \cos^2 \theta (2\omega \cos \theta + \sin \theta) ((k-1)\omega \cos \theta + k \sin \theta)}{32\omega^4}, \\ \dot{\theta} &= -\omega + \frac{r \cos \theta (\cos \theta - 2\omega \sin \theta) ((k-1)\omega \cos \theta + 2k \sin \theta)}{8\omega^2} \\ &\quad - \frac{kr^2 \cos^2 \theta (\cos \theta - 2\omega \sin \theta) ((k-1)\omega \cos \theta + k \sin \theta)}{32\omega^4}. \end{aligned}$$

Now we take as new independent variable in the defferential system (16) the angle  $\theta$  and we expand  $\frac{dr}{d\theta}$  in power series of  $r$  at  $r = 0$  and we obtain that

$$(17) \quad \begin{aligned} \frac{dr}{d\theta} = & -\frac{r^2 \cos \theta (2\omega \cos \theta + \sin \theta) ((k-1)\omega \cos \theta + 2k \sin \theta)}{8\omega^3} \\ & -r^3 \left( \frac{k \cos^2 \theta (2\omega \cos \theta + \sin \theta) ((k-1)\omega \cos \theta + k \sin \theta)}{32\omega^5} + \right. \\ & \left. \frac{\cos^2 \theta (2\omega \cos \theta + \sin \theta) (\cos \theta - 2\omega \sin \theta) ((k-1)\omega \cos \theta + 2k \sin \theta)^2}{64\omega^6} \right) \\ & + O(r^4). \end{aligned}$$

In order to compute the first return map in a neighborhood of the origin of coordinates from the half-axis  $x > 0$  into itself we shall compute the first terms of the solution

$$(18) \quad r(\theta) = v_1(\theta)r_0 + v_2(\theta)r_0^2 + v_3(\theta)r_0^3 + O(r_0^4), \quad \text{such that } r(0) = r_0.$$

This solution starts at the point  $(r_0, 0)$  of the half-axis  $x > 0$  with  $r_0 > 0$  sufficiently small.

As usual we denote by  $r'(\theta)$  the derivative of  $r(\theta)$  with respect to  $\theta$ . Then substituing  $r(\theta)$  from (18) into (17) we obtain

$$\begin{aligned} v_1'(\theta)r_0 + & \left( \frac{\cos \theta (2\omega \cos \theta + \sin \theta) ((k-1)\omega \cos \theta + 2k \sin \theta) v_1(\theta)^2}{8\omega^3} + v_2'(\theta) \right) r_0^2 \\ + & \left( \left( \frac{k \cos^2 \theta (2\omega \cos \theta + \sin \theta) ((k-1)\omega \cos \theta + k \sin \theta)}{32\omega^5} + \right. \right. \\ & \left. \left. \frac{\cos^2 \theta (2\omega \cos \theta + \sin \theta) (\cos \theta - 2\omega \sin \theta) ((k-1)\omega \cos \theta + 2k \sin \theta)^2}{64\omega^6} \right) v_1(\theta)^3 + \right. \\ & \left. \frac{\cos \theta (2\omega \cos \theta + \sin \theta) ((k-1)\omega \cos \theta + 2k \sin \theta) v_1(\theta) v_2(\theta)}{4\omega^3} + v_3'(\theta) \right) r_0^3 + O(r_0^4) = 0. \end{aligned}$$

Thus we must have  $v_1'(\theta) = 0$ , and since  $r(0) = r_0$ , i.e.  $v_1(0) = 1$ ,  $v_2(0) = 0$ ,  $v_3(0) = 0, \dots$  So we must take  $v_1(\theta) = 1$ . We determine the functions  $v_2(\theta)$  and  $v_3(\theta)$  in such a way that the coefficients of  $r_0^2$  and  $r_0^3$  vanish. Thus solving the linear differential equation

$$\frac{\cos \theta (2\omega \cos \theta + \sin \theta) ((k-1)\omega \cos \theta + 2k \sin \theta)}{8\omega^3} + v_2'(\theta) = 0,$$

with the initial condition  $v_2(0) = 0$ , we obtain the function  $v_2(\theta)$  that satisfies that  $v_2(2\pi) = 0$ , so the second Liapunov constant is zero. We do not provide the explicit long expression of the function  $v_2(\theta)$ .

Now we compute the function  $v_3(\theta)$  solving the linear differential equation

$$\begin{aligned} & \frac{k \cos^2 \theta (2\omega \cos \theta + \sin \theta) ((k-1)\omega \cos \theta + k \sin \theta)}{32\omega^5} + \\ & \frac{\cos^2 \theta (2\omega \cos \theta + \sin \theta) (\cos \theta - 2\omega \sin \theta) ((k-1)\omega \cos \theta + 2k \sin \theta)^2}{64\omega^6} + \\ & \frac{\cos \theta (2\omega \cos \theta + \sin \theta) ((k-1)\omega \cos \theta + 2k \sin \theta) v_2(\theta)}{4\omega^3} + v_3'(\theta) = 0, \end{aligned}$$

with the initial condition  $v_3(0) = 0$ . Again the expression of  $v_3(\theta)$  is huge and we do not provide it. Finally the third Liapunov constant

$$V_3 = v_3(2\pi) = -\frac{\pi(2k-1)(2(k-1)\omega^2 + k)}{128\omega^5}.$$

This Liapunov constant written in the original parameters  $b$  and  $c$  is

$$V_3 = \frac{\pi c^{5/2} (b(-4(b-1)^{3/2}\sqrt{c} + b - 2) + 1) (b^2 - 2b((b-1)^{3/2}\sqrt{c} + 1) + 1)}{4((b-1)^{3/2}\sqrt{c} - 2(b-1)bc)^{5/2}}.$$

Moreover, using (12) we obtain that  $V_3 < 0$ . Therefore a stable limit cycle bifurcates from the equilibrium point  $p_+$  for values of  $d < d_0$  but sufficiently close to  $d_0$ . This completes the proof of Theorem 2.

#### 4. PHASE PORTRAITS IN THE POINCARÉ DISC

We note that from Proposition 4 the local phase portraits at the infinite equilibria are independent of the values of the parameters of the differential system (6).

**4.1. Phase portrait for  $1 - 4b(c+d) < 0$ .** Taking into account the following three things: first from Proposition 3 system (6) has only one finite equilibrium point which is a stable node, second the local phase portraits at the infinite equilibria from Proposition 4, and third that the straight line  $x = 0$  is invariant for the system (6), it follows that there is a unique possible global phase portrait in the Poincaré disc given in Figure 1(a). This phase portrait is realized for the values of the parameters  $b = c = d = 1$ .

**4.2. Phase portrait for  $1 - 4b(c+d) = 0$ .** As in the previous case taking into account the same three things, but now from Proposition 3 system (6) has two finite equilibrium points a stable node and a saddle-node, there is a unique possible global phase portrait in the Poincaré disc given in Figure 1(b). We recall that in this case the system cannot have limit cycles because a limit cycle must surround some equilibrium point, and it cannot surround the origin which is on the invariant straight line  $x = 0$  and cannot surround the saddle-node which has topological index zero, because the sum of the indices of the equilibria surrounded by a limit cycle must be one, see for more details Chapter 6 of [7]. This phase portrait is realized for the values of the parameters  $b = 1/4$  and  $c = d = 1/2$ .

**4.3. Phase portraits for  $1 - 4b(c + d) > 0$ .** In this case system (6) has three finite equilibrium points, a stable node, a saddle and the third equilibrium point has, using Theorem 2 and Proposition 3, three possibilities either a node, or a focus surrounded or not by a unique limit cycle assuming that the conjecture holds.

*Case 1:* When the third finite equilibrium point is a stable node or a stable focus non-surrounded by limit cycles a unique phase global phase portrait in the Poincaré disc can be obtained as in the subcase 4.1, see Figure 1(c). For instance this phase portrait is realized for the values of the parameters  $b = c = d = 1/4$ .

*Case 2:* When the third finite equilibrium point is an unstable node or focus with  $d > d_0$  and a stable separatrix of the saddle comes from that third equilibrium, the unique possible global phase portrait in the Poincaré disc is the one described in Figure 1(d). This phase portrait is realized for the values of the parameters  $b = 1/13$ ,  $c = 1/100$  and  $d = 129245/1000000 > d_0$ .

*Case 3:* When the third finite equilibrium point is a stable focus surrounded by an unstable limit cycle which has born in a Hopf bifurcation, see Theorem 2, the unique possible global phase portrait in the Poincaré disc is the one described in Figure 1(e). This phase portrait is realized for the values of the parameters  $b = 1/13$ ,  $c = 1/100$  and  $d = 1292/10000 < d_0$ .

*Case 4:* When the third finite equilibrium point is a stable focus and the unstable limit cycle which had born in a Hopf bifurcation disappears in a loop of the saddle, the unique possible global phase portrait in the Poincaré disc is the one described in Figure 1(f). This phase portrait is realized for the values of the parameters  $b = 1/13$ ,  $c = 1/100$  and  $d = d^*$  for some  $d^* \in (1/10, d_0)$ . A such  $d^*$  exists by continuity moving the parameter  $d$  between the Cases 3 and 5.

*Case 5:* When the third finite equilibrium point is a stable focus and an unstable separatrix of the saddle goes to the stable focus, the unique possible global phase portrait in the Poincaré disc is the one described in Figure 1(g). This phase portrait is realized for the values of the parameters  $b = 1/13$ ,  $c = 1/100$  and  $d = 1/10$ .

This completes the proof of Theorem 1.

#### ACKNOWLEDGMENTS

The first author is partially supported by the Ministerio de Ciencia, Innovación y Universidades, Agencia Estatal de Investigación grants MTM2016-77278-P (FEDER) and PID2019-104658GB-I00 (FEDER), the Agència de Gestió d'Ajuts Universitaris i de Recerca grant 2017SGR1617, and the H2020 European Research Council grant MSCA-RISE-2017-777911. The second author is partially supported by the Algerian Ministry of Higher Education and Scientific Research.

#### REFERENCES

- [1] P. AFFANDI, FAISAL, *Optimal control mathematical SIR model of malaria spread in South Kalimantan*, IOP Conf. Series: Journal of Physics: Conf. Series1116 (2018) 022001.
- [2] F. BRAUER, C. CASTILLO-CHAVEZ, *Mathematical Models in Population Biology and Epidemiology*, Springer, New York, NY, USA, 2000.
- [3] N. S. BARLOW, S. J. WEINSTEIN, *Accurate closed-form solution of the SIR epidemic model*, Physica D 408 (2020) 132540.

- [4] L. CHEN L, J. CHEN, *Nonlinear biological dynamic systems.*, Beijing: Science; 1993. [in Chinese].
- [5] I. COOPER , A. MONDAL , C. G. ANTONOPOULOS, *A SIR model assumption for the spread of COVID-19 in different communities*, Chaos, Solitons and Fractals 139 (2020) 110057.
- [6] O. DIEKMANN, J. A. P. HEESTERBEEK, *Mathematical Epidemiology of Infectious Diseases*, John Wiley Sons, Chichester, UK, 2000.
- [7] F. DUMORTIER, J. LLIBRE, J.C. ARTÉS,, *Qualitative Theory of Planar Differential Systems*, UniversiText, Springer-Verlag, New York, 2006.
- [8] W.O. KERMACK, A.G. MCKENDRICK, A contribution to the mathematical theory of epidemics, Proc. Roy. Soc. A 115 (1927) 700–721.
- [9] Y.A. KUZNETZOV, *Elements of applied bifurcation theory*, second editions, Appl. Math. Sci. **112**, Springer, New York, 1998.
- [10] W.M. LIU, S.A. LEVIN, Y. LWASA, *Influence of nonlinear incidence rates upon the behavior of SIRS epidemiological models*, J. Math. Biol. (1986), 187–204.
- [11] W.M. LIU, H.W. HETHCOTE, S.A. LEVIN, *Dynamical behavior of epidemiological models with nonlinear incidence rates*, J Math. Biol. **25** (1987), 359–380.
- [12] A.K. MISRA, V. SINGH, *A delay mathematical model for the spread and control of water borne diseases*, J. Theor. Biol. **301**, (2012) 49–56
- [13] K.S. SHAROV, *Creating and applying SIR modified compartmental model for calculation of COVID-19 lockdown efficiency*, Chaos, Solitons and Fractals 141 (2020) 110295.
- [14] V. VOLPERT, M. BANERJEE, S. PETROVSKII, *On a quarantine model of coronavirus infection and data analysis*, Math. Model. Nat. Phenom. 15 (2020) 24.
- [15] H. WANG, *Existence of Hopf bifurcation periodic solution to SIRS epidemiological models with nonlinear incidence rates*, J. Anhui. Agric. Univ. **29** No 2 (2002), 199–202 (in Chinese).
- [16] G.Z. ZENG, L.S. CHEN, L.H. SUN, *Complexity of an SIR epidemic dynamics model with impulsive vaccination control*, Chaos, Solitons and Fractals **26** (2005) 495–505

<sup>1</sup> DEPARTAMENT DE MATEMÀTIQUES, UNIVERSITAT AUTÒNOMA DE BARCELONA, 08193 BELLATERRA, BARCELONA, CATALONIA, SPAIN

*Email address:* jllibre@mat.uab.cat

<sup>2</sup> DÉPARTEMENT DE MATHÉMATIQUES, UNIVERSITÉ DE BORDJ BOU ARRÉRIDJ, BORDJ BOU ARRÉRIDJ 34265, EL ANASSER, ALGERIA

*Email address:* t.salhi@univ-bba.dz